PHYSICAL REVIEW A VOLUME 44, NUMBER 8 15 OCTOBER 1991

ARTICLES

Noise-induced transitions at a Hopf bifurcation in a first-order delay-differential equation

André Longtin
Complex Systems Group and Center For Nonlinear Studies, Los Alamos National Laboratory, Los Alamos, New Mexico 87545
(Received 15 April 1991)

The influence of colored noise on the Hopf bifurcation in a first-order delay-differential equation (DDE), a model paradigm for nonlinear delayed feedback systems, is considered. First, it is shown, using a stability analysis, how the properties of the DDE depend on the ratio R of system delay to response time. When this ratio is small, the DDE behaves more like a low-dimensional system of ordinary differential equations (ODE's); when R is large, one obtains a singular perturbation limit in which the behavior of the DDE approaches that of a discrete time map. The relative magnitude of the additive and multiplicative noise-induced postponements of the Hopf bifurcation are numerically shown to depend on the ratio R. Although both types of postponements are minute in the large-R limit, they are almost equal due to an equivalence of additive and parametric noise for discrete time maps. When R is small, the multiplicative shift is larger than the additive one at large correlation times, but the shifts are equal for small correlation times. In fact, at constant noise power, the postponement is only slightly affected by the correlation time of the noise, except when the noise becomes white, in which case the postponement drastically decreases. This is a numerical study of the stochastic Hopf bifurcation, in ODE's or DDE's, that looks at the effect of noise correlation time at constant power. Further, it is found that the slope at the fixed point averaged over the stochastic-parameter motion acts, under certain conditions, as a quantitative indicator of oscillation onset in the presence of noise. The problem of how properties of the DDE carry over to ODE's and to maps is discussed, along with the proper theoretical framework in which to study nonequilibrium phase transitions in this class of functional differential equations.

PACS number(s): 05.70.Fh, 02.50.+s, 05.90.+m, 87.10.+e

I. INTRODUCTION

The past two decades have seen a burst of interest in the dynamics of nonlinear delay-differential equations (DDE's). The main applications of DDE's have been to the fields of laser optics [1,2] (to optical bistability in particular), to population biology [3], and to mathematical physiology [4] where they serve as models of physiological control systems. The fact that a DDE in one variable actually describes a time evolution in an infinite-dimensional functional (Banach) space has interesting consequences. For one, such a DDE can undergo a Hopf bifurcation, a property that requires at least two degrees of freedom in an autonomous system of ordinary differential equations (ODE's). In fact, the number of degrees of freedom in such a DDE is roughly on the order of the ratio R of delay to response time, at least in the chaotic regime [5–7]. When this ratio is small, the behavior of the DDE is well approximated by that of the ODE obtained when the delay is set to zero. On the other hand, when the ratio is large, the DDE behaves in certain regards like a one-dimensional discrete-time map [7,8–11].

This paper focuses on the dynamics of stochastic first-order DDE's in the vicinity of a Hopf bifurcation for a range of magnitudes of the ratio R. We draw our motivation mainly from recent experimental and modeling studies of the human pupil light reflex, in which the behavior of solutions of first-order DDE's in the presence of high-intensity colored noise has been a major focus. By increasing the feedback gain of this reflex using an optical method in combination with controllable external electronic feedback, it is possible to induce pupillary oscillations [12,13]. A deterministic theory [14] predicts that a Hopf bifurcation occurs as the gain or delay are increased, in the same way the Ikeda and Mackey-Glass equation bifurcates to a limit cycle. The observed limit cycles, however, are very noisy. By bringing the system near a bifurcation, it is possible to study the nature of this noise more closely because it then dominates the dynamics [13]. In fact, Ref. [13] has shown that much of the irregular fluctuations could be attributed to band-limited noise driving the reflex. These studies have further demonstrated that noise-induced transitions are possible in first-order DDE's, in the sense that the Hopf bifurcation is postponed by either additive or multiplicative noise.

These results need to be extended for two main reasons: (1) an understanding of the origin of the shift and of its dependence on system parameters, especially the delay, can yield useful insights into the quasi-non-

existent theory of stochastic DDE's, and (2) from an experimental point of view, it is important to be able to establish from measurements whether fluctuations in delayed feedback systems are due to additive or multiplicative noise, and to determine, in either case, what the characteristics of the noise are. The present study, therefore, aims to clarify what influence these noise characteristics have on the solutions of DDE's. Further, since there exists no equivalent of Fokker-Planck analysis for stochastic DDE's (see Sec. II), we resort to numerical simulation to understand how the noise interacts with the other time scales of the equations, especially near bifurcation points. Insight into which kinds of analyses can increase our understanding of stochastic DDE's will be obtained by comparing their behavior to that of stochastic ODE's and maps, for which there exists a theory, and to which the DDE reduces when the ratio R is, respectively, small and large.

In this paper we look at the postponement of the Hopf bifurcation by noise in first-order DDE's, and, in particular, on how this effect depends on (1) whether the noise is additive or multiplicative, (2) the correlation time of the noise, and (3) the ratio R. Section II further motivates our work by giving a brief review of noise-induced transitions at a Hopf bifurcation and of what is known about stochastic DDE's. Section III looks at the Hopf bifurcation in DDE's (here and throughout the paper, first-order DDE's are always assumed) as a function of the ratio R, and illustrates how one stability diagram can be used for all values of R. Section IV focuses on the behavior of an order parameter characterizing the stochastic Hopf bifurcation. In particular, the relative magnitude of the postponement for additive and multiplicative noise is studied. Section V investigates the effect of noise correlation time on the postponement, and Sec. VI discusses the effect of noise on the map obtained in the singular limit of the DDE. Section VII studies how the postponement can be predicted by looking at the behavior of a specific quantity, and the paper concludes with a discussion in Sec. VIII.

II. BACKGROUND

For stochastic ODE's, the analysis of the influence of noise on the Hopf bifurcation can be done in principle by studying the associated Fokker-Planck equation, which deterministically specifies the evolution of a probability density in the state variables [15,16]. Methods using normal-form transformations, followed by center manifold reductions either on the stochastic equations [17] or on the Fokker-Planck equation [18], have been used to simplify Fokker-Planck equations. Most of the earlier studies have considered only the case of the Hopf bifurcation with additive noise, and can be extended in principle to the more difficult case of multiplicative noise [17–19]. In the case of a Hopf bifurcation with multiplicative noise, it has been shown that care must be taken to perform the normal-form transformations on the original stochastic system of ODE's [20]. Often, when azimuthal symmetry is not present, adiabatic elimination is performed in order to obtain an approximate analytical solution to the Fokker-Planck equation in which the density depends only on the radial component [17–19,21,22]. The extrema of this one-dimensional probability density can then be investigated as a function of the parameters of the equation and of the noise. In this context the Hopf bifurcation occurs when the density goes from unimodal to bimodal, and the distance between the peaks serves as an order parameter for the bifurcation (see Fig. 1).

One of the first studies of the Hopf bifurcation with noise was by Kabashima and Kawakubo [23], who showed both experimentally using a parametric oscillator and analytically that Gaussian white noise postpones the Hopf bifurcation. Most theoretical studies since have considered the influence of noise on the bifurcation parameter [20,24] and have shown that postponements are possible, although two studies have predicted advancements [21,25]. In Ref. [21], it was shown that whether postponements or advancements occur depends on the relative magnitude of the radial relaxation time onto the limit cycle, the period of rotation in the azimuthal direction, and the noise correlation time. Analog simulations of the Brusselator have revealed only postponements, with advancement effects showing up as decreases in postponement effects for the predicted ranges of the three time scales [26]. This work has proposed, based on an earlier study [27], a rigorous criterion for oscillation onset that allows for possible azimuthal asymmetry of the solution.

Previous work [13] and the present work focus on the following model equation for delayed negative feedback:

$$\frac{dx}{dt} = -\alpha x(t) + f(x(t-\tau)) = c\frac{\theta^n}{\theta^n + x^n(t-\tau)} + k \tag{1}$$

where the noise is on c (multiplicative) or on k (additive), and the bifurcation parameter n controls the slope of the feedback function. The previous study considered invariant densities in one variable for this infinite-dimensional system and found that these have many features in common with those for systems of ODE's such as the Brusselator [26]. Noise-induced transitions were shown to occur in this first-order DDE with either additive or multiplicative colored noise. This is interesting because noise-induced transitions are not possible in a first-order ODE with additive white noise [15]. They have been reported, however, in a two-dimensional system with white noise [28], and in a one-dimensional system with dichotomous colored noise [29]. In particular, Ref. [13] looked at the effect on the Hopf bifurcation of noise correlation time, keeping noise intensity constant but not total noise power. Under these conditions, noise intensity and correlation time have similar effects on the postponement, as was found in Ref. [26].

Understanding these results is important for the development of a theory of stochastic DDE's. The very few results on stochastic DDE's deal mainly with the convergence of a process to a diffusion process satisfying an appropriate stochastic DDE [30]. To our knowledge, only existence proofs for periodic solutions for restricted

classes of stochastic DDE's have been given [31], while uniqueness and stability have not been determined. In fact, the usual Fokker-Planck analysis is *a priori* not possible for a DDE subjected to colored noise, because DDE's are non-Markovian, and so are systems with colored noise (although this problem can be solved, in principle, by introducing an extra variable in the Fokker-Planck analysis).

Understanding the aforementioned results is also important for the identification of noise sources in neural control systems and in particular for determining their power spectra. For example, it is not clear whether noise is injected quasiwhite or colored into the pupil light reflex, since in either case the noise is filtered by the low pass characteristic of the neuromuscular system and manifests itself in pupil area measurements as a band-limited power spectrum. Also, it is not possible to distinguish between the effects of additive and multiplicative noise. Thus, this paper investigates the effect of the correlation time of both additive and multiplicative noise keeping the total power of the noise constant.

III. DETERMINISTIC CASE

The Hopf bifurcation theorem for DDE's is basically the same as for ODE's, except that its proof requires sophisticated techniques from the theory of functional differential equations. Thus there exists a surface of periodic solutions in a two-dimensional center manifold which has quadratic tangency with the eigenspace associated with the eigenvalues $\lambda(n_0),\bar{\lambda}(n_0)$, where n_0 is the parameter value at which the bifurcation occurs. In the

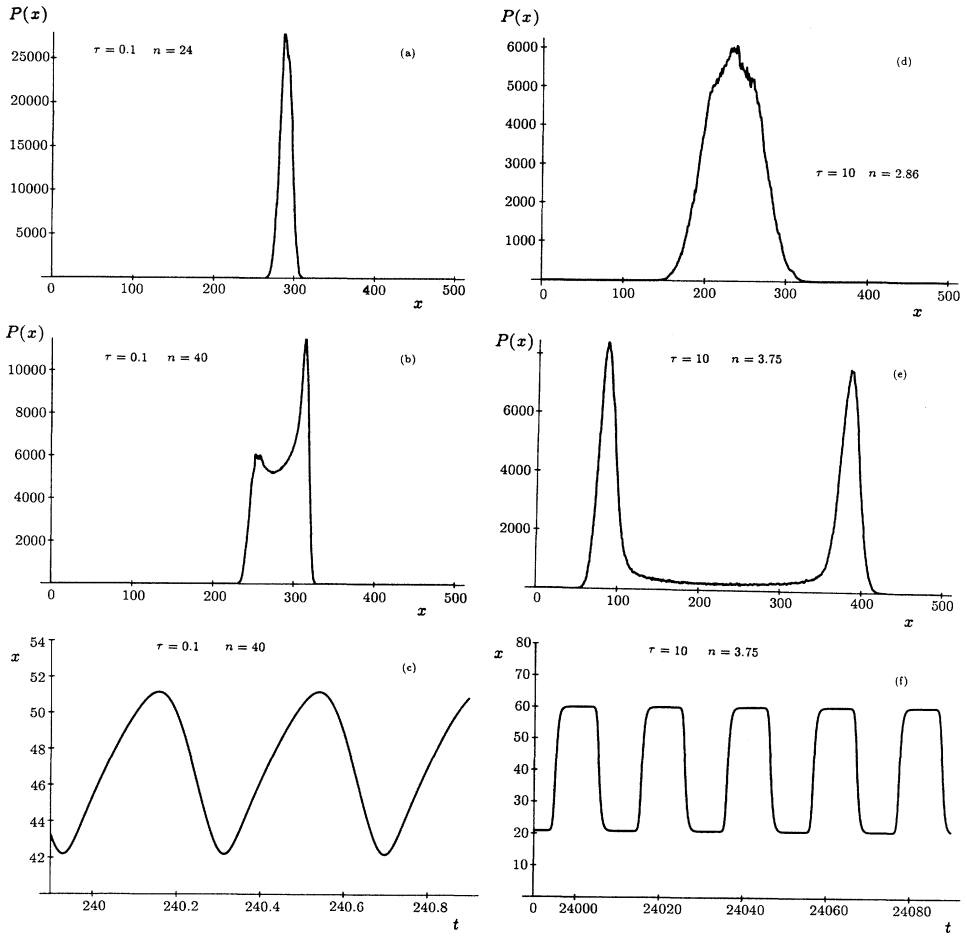

FIG. 1. (a) and (b) Probability densities obtained from numerical integration of Eq. (1) with additive noise for a delay $\tau=0.1$ at values of the parameter n greater than that at which the deterministic Hopf bifurcation occurs ($n_0=22$): (a) $n=24$; (b) $n=40$. (c) Time series without noise corresponding to $n=40$. (d) and (e) are probability densities obtained for $\tau=10$ and values of $n > n_0=2.84$: (d) $n=2.86$; (e) $n=3.75$. (f) time series without noise corresponding to $n=3.75$. The solutions in (c) and (f) should be compared to the quasisinusoidal solution for n near but greater than n_0. The integration time step is $\tau/100$ and the noise correlation time is $t_c=1$ sec. The parameter values are $\alpha=3.21$, $\theta=50$, $c=200$, and $k=0$. The densities $P(x)$ were constructed by dividing the interval [10,75] into 500 bins. The solution was integrated for 2500 delays without noise, and for another 2500 delays with noise before the densities were constructed from the subsequent integration over 10 000 delays. The initial condition was chosen to be a constant on $(-\tau,0)$, which differed by $\approx 1\%$ from the deterministic fixed point.

absence of noise there are two time scales of interest: (1) the azimuthal rotation period and (2) the radial relaxation time onto the limit cycle (see below). The bifurcation of interest in this paper is supercritical, a fact we have verified numerically rather than by carrying out the tedious calculations involved in asserting that nondegeneracy conditions are satisfied [32].

If time is rescaled in units of τ, Eq. (1) becomes

$$\frac{dx}{dt} = -\alpha\tau x(t) + \tau f(x(t-1)) \ . \tag{2}$$

The limit where $R \equiv \alpha\tau \to \infty$ is called the singular perturbation limit. In this limit, the differential term acts as a perturbation on the difference equation that results when this term is not present [33]:

$$x(t) = \alpha^{-1} f(x(t-1)) \ . \tag{3}$$

Equation (3) can be interpreted as a discrete time map (one unit of time being equal to one delay). The dynamical behaviors of this map, such as period-doubling bifurcations and chaotic motion, are also found in the DDE. In fact, the DDE exhibits a much broader range of dynamical behaviors than the map obtained in the singular limit, and is often found to exhibit multistability even when its limiting map does not [7,8,11]. In general, there is no continuous transition between the dynamical structures of the map (periodic orbits, their stability properties, bifurcation points) and those of the DDE, no matter how large the parameter $\alpha\tau$ [9].

Figure 2 plots the Hopf-bifurcation parameter as a function of limit-cycle amplitude at different values of the delay. A fixed-step fourth-order Runge-Kutta method with linear interpolation for the delayed argument was used. The limit-cycle amplitude was computed after integrating the DDE for 5000 delays with an integration time step equal to $\tau/100$. Since α is kept constant, each curve corresponds to a different value of the ratio R (α is kept constant throughout our study). Because of the scales used, the bifurcation curve for the map in Eq. (3) overlaps the $\tau = 10$ curve; in fact, the former is lower (bifurcation at $n_0 = 2.84$) than the $\tau = 10$ curve ($n_0 = 2.853$). A continuous progression is seen between the curves as the ratio R undergoes a 100-fold increase. In the map limit, the Hopf bifurcation becomes, in fact, a standard period-doubling bifurcation (see below). Also, the limit-cycle amplitude increases faster and reaches higher values at higher delays; the limit-cycle amplitude is greatest for the map, and is given by c/α if $k < \alpha\theta < c + k$. In the limit of large n, the limit cycles are as in Fig. 1(c) for $\tau = 0.1$ and in Fig. 1 (f) for $\tau = 10$.

The bifurcation curves in Fig. 2 were obtained by fitting the simulation results to a function of the form

$$n(A) = c_0 + c_1 A^2 + c_2 A^4 + c_3 A^6 \ , \tag{4}$$

where A is the limit-cycle amplitude and n is the bifurcation parameter. This form is dictated by the equation for the radial component in the normal form for the supercritical Hopf bifurcation (see Guckenheimer and Holmes). In doing so, the amplitude of the limit-cycle oscillation is assumed proportional to this radial component.

There is a direct connection between the Hopf bifurcation in a DDE and the first period-doubling (pitchfork) bifurcation in the map obtained in the singular limit of this DDE. A similar connection was made previously in Ref. [10]. Consider the DDE in Eq. (1) and the corresponding map Eq. (3) obtained in the singular limit of Eq. (1). Both these equations have the same fixed point x^*,

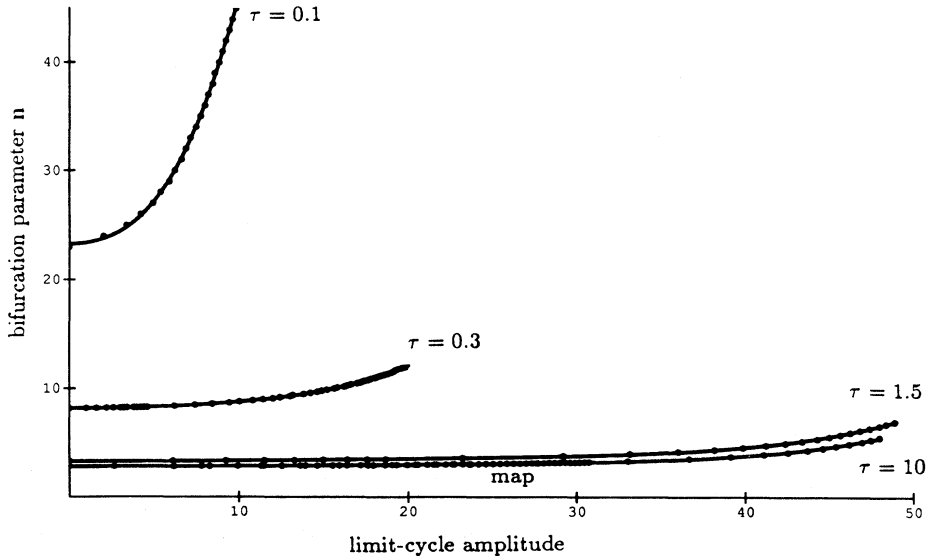

FIG. 2. Limit-cycle amplitude vs the bifurcation parameter n for Eq. (1) in the absence of noise at different delay values: $\tau = \infty$ (map), 10, 1.5, 0.3, and 0.1 sec. In this sequence, the behavior of the DDE in Eq. (1) changes from maplike to ODE-like. The amplitudes were computed after 5000 delays had elapsed with an integration time step of $\tau/100$. From Eq. (6), the Hopf bifurcation occurs at $\tau = 0.1$: $n_0 = 23.45$; $\tau = 0.3$: $n_0 = 8.18$; $\tau = 1.5$: $n_0 = 3.34$; $\tau = 10$: $n_0 = 2.853$; $\tau = \infty$ (map): $n_0 = 2.84$.

which satisfies $x^*=\alpha^{-1}f(x^*)$. The characteristic equation for the DDE (linearized around x^*) is

$$\lambda+\alpha-\beta e^{-\lambda\tau}=0 , \tag{5}$$

where $\beta\equiv f'(x^*)<0$. The rightmost complex-conjugate pair of roots of Eq. (5) lies in the right-hand plane if

$$\omega\tau>\cos^{-1}\left[-\frac{\alpha}{\beta}\right] , \tag{6}$$

where $\omega=(\beta^2-\alpha^2)^{1/2}$ and the inverse cosine takes its value in the interval $[\pi/2,\pi]$. Equality holds in Eq. (6) when the eigenvalues are pure imaginary, at which point the period of the oscillation is given exactly by ω. Defining $B\equiv-\beta$ and $X\equiv-\alpha/B<0$ (since $\alpha>0$), Eq. (6) can be written as

$$\alpha\tau>\frac{\cos^{-1}(X)}{\sqrt{(1/X)^2-1}} . \tag{7}$$

A plot of the stability of the fixed point as a function of $\alpha\tau$ and X is shown in Fig. 3. If $X<-1$ or $X>1$, the fixed point is stable; these regions are labeled "S." Further, the unstable solutions of Eq. (1) occur when inequality Eq. (6) is satisfied; these unstable solutions are found in the regions labeled "U."

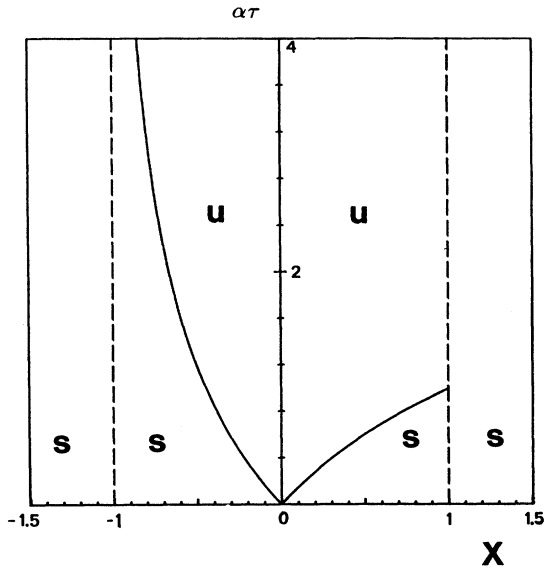

FIG. 3. Stability diagram for the Hopf bifurcation in the first-order DDE Eq. (1). The rightmost conjugate pair of roots of the characteristic equation [Eq. (5)] of Eq. (1) has a negative real part in the regions labeled S and a positive real part in those labeled U. The abscissa is $X\equiv-\alpha/B$ and is negative for smooth negative feedback. For $-1<X<1$, the stability curve that separates the U and S regions and corresponding to the right-hand side of Eq. (7) is plotted as a function of X. For X values in this interval, the singular limit $\alpha\tau\gg1$ of Eq. (1) implies that the inequality in Eq. (6) is always satisfied, and hence the system lies in region U. In this limit, the stability diagram of the DDE collapses down to the X axis, which is the stability diagram for the map Eq. (3). This map undergoes a period-doubling bifurcation at $X=-1$ and a tangent bifurcation at $X=1$.

The onset of oscillatory motion in the map Eq. (3) occurs at the first pitchfork (or "period-doubling") bifurcation, at which $\alpha^{-1}f'(x^*)=-1$ (corresponding to $B/\alpha=1$). The fixed point also loses stability when $\alpha^{-1}f'(x^*)=1$ (or $B/\alpha=-1$), at which a tangent bifurcation occurs. In fact, for $-1<B/\alpha<1$, the fixed point of the map is stable. Since $1/X=-B/\alpha$, both the map and the DDE have a stable fixed point over the same values of X, i.e., for X outside the interval $[-1,1]$. Hence, the stability diagram for the map simply consists of the x axis in Fig. 3. The condition $X=-1$ corresponds to the period-doubling bifurcation in the map, while $X=1$ corresponds to the tangent bifurcation.

When the fixed point is unstable for the map, i.e., for $-1<X<1$, the fixed point of the DDE can be either stable or unstable, depending on the value of $\alpha\tau$. The fact that the map is obtained formally by taking the limit $\alpha\tau\to\infty$ in the DDE implies that only region "U" is relevant for the map. Hence, when $-1<X<0$ for the map, there is always a stable period-2 solution. The stability diagram for the DDE is then seen as a simple prolongation in two dimensions (along the $\alpha\tau$ axis) of the one-dimensional diagram for the map.

As R goes to zero, the Hopf bifurcation in the DDE will occur for a stronger (more negative) slope at the fixed point. Since the maximum and the minimum of the feedback function are fixed, this means that the bifurcation occurs only when the system is very nonlinear, i.e., when the feedback approximates what is known as piecewise constant negative feedback (the function appears as a step decreasing from left to right going from the value $f=c+k$ to $f=k$). As long as the delay is finite, the slope of the feedback function at the fixed point can always be made large enough to cause the system to become unstable and a limit cycle to appear. However, in the limit where the delay goes to zero, the period and the amplitude of the limit cycle can be shown to go to zero [13]. In fact, if the delay goes to zero, equality will hold in Eq. (6) only if $\beta\to-\infty$, and the period $T=2\pi/\omega$ will go to zero since $\omega=(\beta^2-\alpha^2)^{1/2}$ becomes infinite. The $\tau\to0$ limit of the Hopf bifurcation in the DDE is thus peculiar since the DDE becomes effectively an ODE with piecewise-constant feedback, although it has a periodic solution, making it equivalent to a two-dimensional ODE; this periodic solution, however, has zero period and amplitude.

At oscillation onset, the period is given by

$$T=\frac{2\pi}{(\beta^2-\alpha^2)^{1/2}} . \tag{8}$$

The other time scale of interest is the radial relaxation time onto the limit cycle, t_r, which can be obtained as follows. The radial component of the normal form [34] of the Hopf bifurcation is to $O(r^3)$:

$$\frac{dr}{dt}=(d\mu+ar^2)r , \tag{9}$$

where the bifurcation parameter μ corresponds in our

case to $n-n_0$ and

$$d \equiv \left. \frac{d\,\mathrm{Re}(\lambda)}{d\mu} \right|_{\mu=\mu_0} . \tag{10}$$

The quantity a determines whether the periodic solution is attracting or not. By linearizing Eq. (9) around the limit-cycle amplitude $r^*=(-d\mu/a)^{1/2}$, one obtains the relaxation time constant $t_r=(2d\mu)^{-1}$. This implies that t_r will be small (the limit cycle will be strongly attracting) if the real part of the complex-conjugate pair of roots of Eq. (5) becomes positive rapidly as μ increases. In our case, setting $B=-\beta$ in Eq. (5), the quantity d is

$$\begin{aligned} d &= \left. \frac{d\,\mathrm{Re}(\lambda)}{dn} \right|_{n=n_0} \\ &= -\left. \frac{d\,\mathrm{Re}(\lambda)}{dB} \right|_{n=n_0} \left. \frac{d\beta}{dn} \right|_{n=n_0} \\ &= \left[\frac{\alpha+B_0^2\tau}{B_0+2\alpha\tau B_0+B_0^3\tau^2} \right] \left[-\left. \frac{d\beta}{dn} \right|_{n=n_0} \right] . \end{aligned} \tag{11}$$

This was obtained by implicitly differentiating Eq. (5) with respect to B and evaluating the result at $\lambda=i\omega_0=i(B_0^2-\alpha^2)^{1/2}$, where $B_0=-\beta(n_0)$. The problem now is in evaluating the quantity $d\beta/dn$, i.e., how the derivative at the fixed point of Eq. (1) varies with n, given that the fixed point varies itself with n and is defined by an analytically intractable implicit equation. It can be shown that

$$f'(x^*)=-\frac{n\alpha^2\theta}{c}\left[\frac{x^*}{\theta}\right]^{n+1} . \tag{12}$$

Using the logarithmic derivative and the fixed-point condition, the following expression is obtained:

$$\frac{d\beta}{dn}=\alpha K+n\alpha K\left[\frac{1+K}{1-nK}\right]\ln\left[\frac{x^*}{\theta}\right] , \tag{13}$$

where $K=-\alpha\theta/c(x^*/\theta)^{n+1}$. Note that this is still an implicit expression since x^* depends on n, but it is the best we can do. Nevertheless, the variation of $d\beta/dn$ is surprisingly almost linear, as shown in Fig. 9. Numerical values at the bifurcation are $\tau=0.1:-0.65$; $\tau=0.3:-0.727$; $\tau=1.5:-0.871$; $\tau=10:-0.907$; $\tau=\infty:-0.2834$. Having obtained B_0 from the same computation, Eq. (11) can be evaluated and the relaxation times in units of the delay are $t_r=k_r/(n-n_0)$, with $\tau=0.1:k_r=18.9$; $\tau=0.3:k_r=6.805$; $\tau=1.5:k_r=2.447$; $\tau=10:k_r=1.838$; $\tau=\infty:k_r=1.765$. In absolute value, t_r is found to increase with the delay, and actually to diverge for $\tau\to\infty$. However, since $(n-n_0)$ is typically larger for $\tau=0.1$ than for $\tau=10$, the relative time constant $k_n/(n-n_0)$ does not vary much with τ.

IV. STOCHASTIC CASE

This section describes the method used to compute the behavior of the order parameter as a function of n, and gives results on the relative magnitude of the additive and multiplicative shifts at two different noise correlation times. The Ornstein-Uhlenbeck (OU) process with correlation time $t_c=\lambda^{-1}$ is the solution of the stochastic differential equation

$$\frac{d\zeta}{dt}=-\lambda\zeta+\lambda\xi(t) \tag{14}$$

in which $\xi(t)$ is a Gaussian white-noise process of zero mean, i.e., $\langle\xi(t)\rangle=0$ and $\langle\xi(t)\xi(s)\rangle=2D\delta(t-s)$. The power spectrum of the OU process with the scaling in Eq. (14) is

$$S(\nu)=\frac{D\lambda^2}{\pi(\lambda^2+\nu^2)} \tag{15}$$

(ν is the frequency) and the two-point correlation function is

$$C(t,s)=\frac{D}{t_c}\exp(-\lambda|t-s|) . \tag{16}$$

The total power in the noise is given by

$$\int_{-\infty}^{\infty} S(\nu)d\nu=\frac{D}{t_c}=C(0) . \tag{17}$$

To our knowledge, there has been no systematic study of the effect of t_c on the Hopf bifurcation at constant noise power D/t_c in ODE's or DDE's. This is done in the next section. The simulations reported in this section are also done for constant total power $C(0)=24.5$, corresponding to $\sigma=\sqrt{2D}=7.0$ when $t_c=1.0$.

The numerical integration of the stochastic DDE is done by coupling the algorithm for the deterministic DDE (Sec. III) to the integral Euler algorithm for the Ornstein-Uhlenbeck process proposed by Fox *et al.* [35]. At each value of n, Eq. (1) is integrated using a constant initial function on $(-\tau,0)$ which differs by $\approx 1\%$ from the deterministic fixed point at the Hopf bifurcation $x^*(n_0)$ [e.g., $x^*(n_0)=44.6$ for $\tau=0.3$]. The solution is first allowed to settle onto the limit cycle in the absence of noise for 2500 delays, at which point noise is applied, and another 2500 delays are discarded as transients. Equation (1) is then further integrated for 20 000 delays during which time the solution is used to construct a 500-bin histogram corresponding to the solution interval (10,75). The order parameter is estimated graphically by measuring the peak separation in this histogram. The error in this procedure, due to the estimation of the position of the maxima, the finite bin size (0.13), and to the inherent statistical fluctuation for this type of stochastic process, is greatest near oscillation onset where the peaks are difficult to resolve. This maximal error for total noise power $\sigma=7$ is approximately $\pm 1\%$, or ± 0.7. This error decreases very quickly with n to reach about one-third of this value. Tests at $\tau=1.5$ for additive noise with $\sigma=15, t_c=1.0$ have revealed statistical fluctuations on the order of 0.5% between the standard simulation described above, and one with half the step size (i.e., $\tau/200$) and with another one with an integration time of 10^5 delays (time step of $\tau/100$).

We have tested the algorithm for the Ornstein-Uhlenbeck noise for Gaussian quality, and found that it behaved satisfactorily at all values of t_c used, even for

$t_c = 10$ using the largest integration time step in our study, 0.1 sec, corresponding to $\tau/100$ when $\tau = 10$. Also, the order parameter for $\tau = 10, t_c = 0.01$ with time step 0.01 sec was found to differ at most from the order parameter computed with half the step size (same total integration time) by ± 0.35 or 0.5%.

The results are shown in Figs. 4 and 5, where the bifurcation parameter n is plotted as a function of the order parameter ("amplitude") for four values of the delay. The simulation results used to determine the fits are superimposed on the fitted curves. In Fig. 4, $t_c = 1$ sec, and the standard deviation of the noise is $\sigma = \sqrt{2D} = 7$ and 15. For $\tau = 0.1$, only the simulations for $\sigma = 7$ are shown, since the noise level $\sigma = 15$ is too high to permit resolving the peaks [note that these peaks are quite close for $\sigma = 7$; see Fig. 1(b)]. The curves are fit in the same way as in Fig. 2, i.e., using Eq. (4). For $\tau = 10$, the differences between the fitted curves and the fitted curve for the deterministic case (the lower curve in the plots at the other delays) are plotted as a function of the bifurcation parameter itself. These differences are thus the vertical distances between the curves and correspond to the shift of the Hopf bifurcation. These differences are very sensitive to the fits, and should not be interpreted too literally at the (low) values of n at which the order parameter starts to grow. Also, because of the uncertainty in the fit at lower values of n, it is not possible to obtain an accurate estimate of the shift by comparing the ordinates of the fitted curves at the origin [i.e., the c_0 values in Eq. (4)].

It is clear from Fig. 4 that the shift is proportional to σ when t_c is kept constant, as reported in earlier studies [13,26]. Also, it is interesting to compare the relative magnitude of the additive and multiplicative shifts as the delay increases. One clearly sees a qualitative change in behavior as τ increases. At small τ, the multiplicative shift is larger than the additive shift, while the opposite holds at large τ, with the crossover occurring near $\tau = 0.3$. This is true at both noise intensities. In the map limit (Sec. VI), the shifts are found to be small and almost of equal magnitude. Thus, once the crossover has occurred, the shifts both decrease with increasing delay until they become equal in the infinite delay limit. In Fig. 5, results are shown for $t_c = 0.01$ and at only one value of noise standard deviation $\sigma = 0.7$, corresponding to the same total power $C(0) = 24.5$ as in Fig. 4. In this case, the additive shift is always greater than the multiplicative one, and the shifts are smaller than in Fig. 4 (the same curves are shown in Figs. 6 and 7 where they are the closest ones to the deterministic curve). Hence the crossover appears to be a feature of larger noise t_c, which suggests that it may also be a property of higher-dimensional stochastic DDE's.

Although noise-induced transitions are still present in the quasiwhite $t_c = 0.01$ case, they are very small, and it is difficult to say with certainty whether they persist at even smaller values of t_c. Analog simulations should be per-

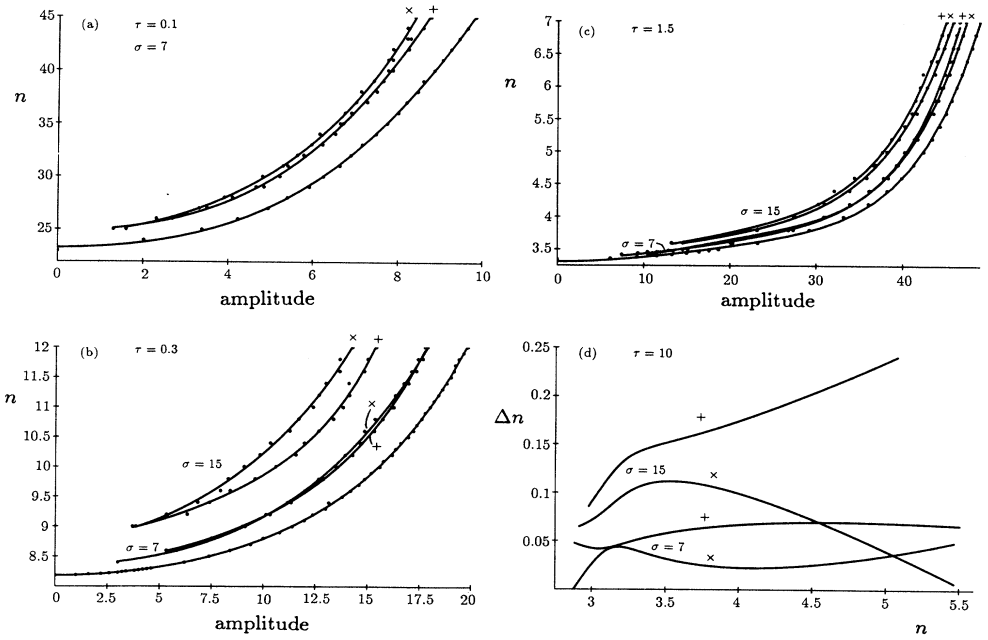

FIG. 4. Bifurcation parameter n as a function of the magnitude of the separation between the peaks (order parameter or "amplitude") in the density of the solution of Eq. (1). The simulations were done for noise correlation time $t_c = 1.0$ sec and standard deviations of $\sigma = 7$ and 15 at four different values of the delay: (a) 0.1, (b) 0.3, (c) 1.5, and (d) 10 sec. For each delay, the points plotted range over values of n for which the peak separation could be measured. Each plot compares the postponed Hopf bifurcation when the noise is additive (on k: "+") or parametric (on c: "X") to the deterministic curve (lowest curve starting at the y axis). Each curve is plotted along with the data points used to fit it to an even polynomial of order 6. Since the curves are difficult to resolve graphically for $\tau = 10$ (d), the difference between the fitted functions, Δn, has been plotted vs n. The parameters are $\alpha = 3.21$, $c = 200$, $k = 0$, $\theta = 50$, and $t_c = 1$ sec. The integration time step is $\tau/100$. Numerical solutions and densities are obtained as in Fig. 1.

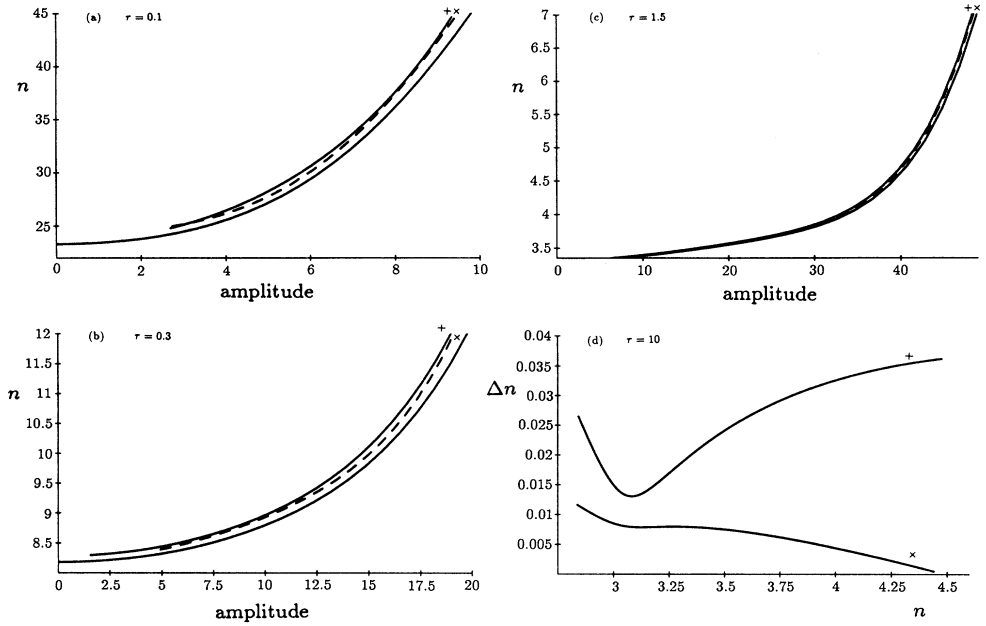

FIG. 5. Bifurcation parameter n vs the magnitude of the order parameter for Eq. (1) as in Fig. 4, but with $t_c = 0.01$ and $\sigma = 7.0$. Again the difference between the fitted functions was plotted vs n for $\tau = 10$.

formed to resolve this question. In any case, it is clear that the shifts are greater at small delays. This is interesting because these simulations at small t_c and small delay are the best conditions under which the DDE could behave as a first-order ODE. However, Fokker-Planck theory predicts that additive noise-induced transitions are not possible in first-order ODE's with Gaussian white noise. This implies that either the shifts should go to zero in the $t_c \to 0$ limit, in accordance with the theory, or that they do not because a DDE undergoing a Hopf bifurcation is never equivalent to a first-order ODE.

Note that additive noise can make f become negative if

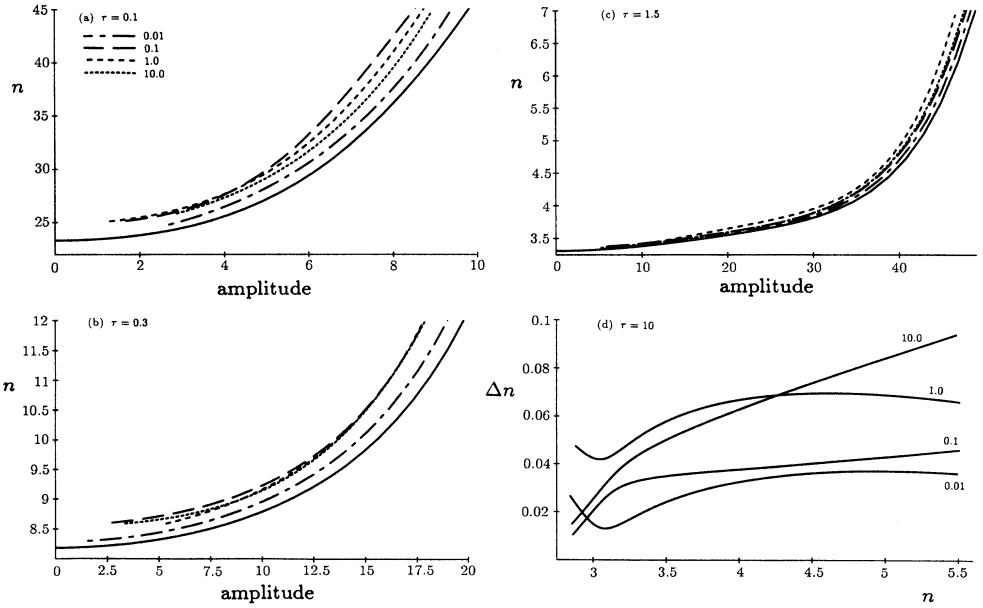

FIG. 6. Bifurcation parameter n vs the magnitude of the order parameter for four values of the noise correlation time and at four values of the delay: (a) 0.1, (b) 0.3, (c) 1.5, and (d) 10 sec. The noise is additive [i.e., on k in Eq. (1)] and its standard deviation is adjusted so as to keep the total power of the noise constant and equal to $C(0) = 24.5$. Each plot compares the bifurcation curve for $t_c = 0.1, 1.0, 10.0$ to that for the deterministic case (solid curve). Numerical integration, provision for transients, and construction of the densities is as in Fig. 1. The correspondence between the curve style and t_c is given in the legend of (a).

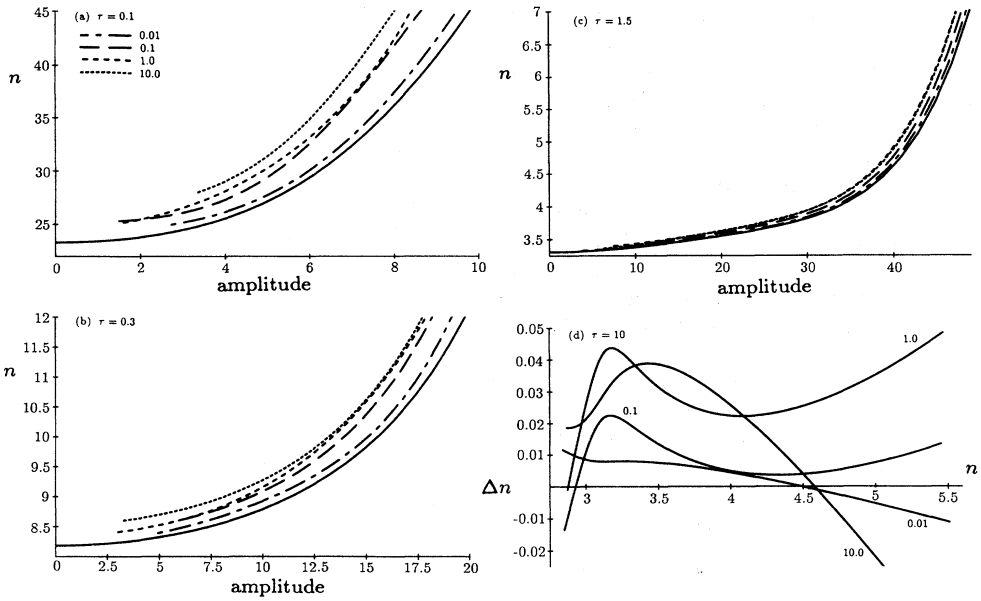

FIG. 7. Bifurcation parameter n vs the magnitude of the order parameter as in Fig. 6 but with multiplicative noise on c in Eq. (1) rather than additive noise.

k is small and the noise amplitude is large. This is not a problem because the computation is done around the unstable fixed point. The fact that $f(x(t-\tau))$ is negative does not imply that x will be negative, since the system is always attracted toward the limit cycle. Also, for large delays, the invariant density becomes strongly peaked as the bifurcation parameter increases, i.e., the ratio of peak height to the minimum between the peaks is very large [compare Figs. 1(b) and 1(e)]. This ratio is proportional to the delay. This is due to the fact that for large delays, the oscillation rapidly changes from a harmonic to a square-wave type in which transitions between the levels occur [10] on a time $O(\alpha^{-1})$.

V. EFFECT OF NOISE CORRELATION TIME

It is important to understand the behavior of the Ornstein-Uhlenbeck (OU) process when taking the $\alpha\tau$ limit of Eq. (1). This limit produces a stochastic process coupled to a finite difference equation. This can be seen by first rescaling time in the coupled DDE-OU system in units of τ, which yields

$$\frac{dy}{dt} = -\alpha\tau y(t) + \tau f(y(\tau-1)) + \tau\eta(t) ,$$
$$\frac{d\eta}{dt} = -\lambda\tau\eta(t) + \lambda\tau\overline{\xi(t)} . \tag{18}$$

If $\alpha\tau \gg 1$, then it follows

$$y(t) \simeq \alpha^{-1} f(y(t-1)) + \alpha^{-1}\eta(t) \tag{19}$$

in which time is still continuous. Furthermore, with this scaling, the correlation of the OU process becomes

$$\langle \eta(t)\eta(s)\rangle = D\lambda\tau e^{-\lambda\tau|t-s|} \tag{20}$$

in which the noise correlation time $t_c = (\lambda\tau)^{-1}$. Hence, as $\tau \to \infty$, $t_c \to 0$ and the noise becomes effectively white with intensity $2D$ as usual.

In this limit also, the DDE has become a continuous time difference equation [in the same way as Eq. (3) before discretizing time in units of the delay]. All the points on an interval $[t, t+\tau]$ are mapped by f in Eq. (3) to points on the interval $[t+\tau, t+2\tau]$, and the points behave independently. This corresponds to doing an infinite number of realizations of the stochastic map in parallel. If one is interested only in the density from which to measure the order parameter, it is clear, if the map is ergodic (as it is in our case), that only one realization suffices to construct this density. As a consequence, the correlation time of the noise is not important for determining the order parameter, although it will certainly determine the precise time solution [7,36].

The effect of additive and multiplicative noises of constant total power but different correlation times is illustrated in Figs. 6 and 7. For additive noise, Fig. 6 shows that, for this 1000-fold range of noise correlation times, postponements of the Hopf bifurcation are to be expected. However, the magnitude of the shift does not seem to follow any clear pattern at any of the delay values investigated, apart from the following two observations: (1) the quasiwhite case $t_c = 0.01$ always produces the smallest shift, and (2) the strongest shift always seems to occur for the noise correlation time that is closest to the delay. In the multiplicative noise case, shifts are again seen across this range of t_c, and further there is a clear pattern: the shift is proportional to t_c. The reasons for this behavior and the patterns observed in the additive noise case are not known, nor is it known whether these patterns depend on the precise choice of values for the other param-

eters, especially of α. For the $\tau=10$ case for both additive and multiplicative noise, the separation between the fitted curves and the deterministic curve has been plotted versus the bifurcation parameter, as in Figs. 4 and 5, again because the fitted curves themselves cannot be resolved adequately. As in Figs. 4 and 5, these curves should not be interpreted too literally, due to the statistical error on the points fitted, but rather they should be thought to give a rough measure of the relative shifts. Hence, the negative values in Fig. 6(d) may be interpreted as advancements, especially those occurring for large n where the precision is higher, but this point must be substantiated by more extensive simulations. Such constant power simulations have not been reported to our knowledge, and thus they may provide insights into the development of a theory for colored noise-induced transitions in DDE's, as in Ref. [21] for ODE's.

VI. EFFECT OF NOISE ON THE MAP $x_{i+1}=\alpha^{-1}f(x_i)$

In this section the influence of noise on the map obtained in the singular limit of Eq. (1),

$$x_{i+1}=(c/\alpha)f(x_i)+k/\alpha \ , \tag{21}$$

is considered. Previous studies [37,38] have looked at the effect of noise on the dynamics of the logistic map. They have found that for such discrete time systems, there is an equivalence between additive and multiplicative noise, in the sense that the effect of an additive perturbation can be mimicked by an appropriately chosen multiplicative perturbation. In their more rigorous analysis, Linz and Lücke [38] have computed this equivalence by equating the moment generating functions for the trajectories x_{n+1} and $\tilde{x}_{n+1}$ influenced, respectively, by multiplicative noise of variance Δ^2 and additive noise of variance $\tilde{\Delta}^2$:

$$\langle \exp(ikx_{n+1})\rangle = \langle \exp(ik\tilde{x}_{n+1})\rangle \ . \tag{22}$$

This results in the relation $\Delta_{\text{add}} \rightarrow [(r-1)/r]\Delta_{\text{mult}}$, where r is the parameter in the logistic map. This implies that additive noise has a slightly stronger influence on the dynamics than multiplicative noise.

Inspection of the proof of this result shows that it should be valid for any single-humped map of the form

$$x_{i+1}=r_1 f(x_i)+r_2 \ , \tag{23}$$

where r_1 and r_2 are parameters subjected to noise. In fact, the identification $r_1 \rightarrow c/\alpha$ and $r_2 \rightarrow k/\alpha$ of the parameters in Eq. (21) with those of the map in Eq. (23) above allows us to extend their result to this map. Then, since $c/\alpha \sim 62$, the ratio $(r-1)/r$ is very close to 1, and thus there should be very little difference between additive and multiplicative noise.

We have in fact found that both shifts are almost equal within statistical error (data not shown). They are, however, very small, occurring between $n=2.85$ and 2.86. Inspection of our bifurcation curves in Figs. 4–7 reveals that the two shifts become smaller as the delay increases, and further the difference between them decreases. One thus sees a clear convergence of the properties of the DDE to those of the map in the presence of noise.

VII. THE ROLE OF $\langle f(x^*)\rangle_\xi$

In this section, we discuss the behavior of one quantity whose changes do correlate well with the onset of oscillation in the presence of noise. The quantity that is most influenced by the noise, whether additive or multiplicative, is the slope of the feedback function at the fixed point, $f(x^*)\equiv\beta$. In our study, this is the only fluctuating quantity in the oscillation condition Eq. (6), and thus one suspects that it may determine the growth of the order parameter. Figure 8 plots the feedback function f in Eq. (1), at a given value of n, versus its argument $x(t-\tau)$ with and without (a) additive and (b) multiplicative noise, as in the simulations presented so far. The dashed lines represent positive and negative perturbations (magnitude equal to 15) to f.

Each perturbation causes the fixed point of the system to change, since this point is determined by the intersection of the line $y(x)=\alpha x$ with $f(x)$, as shown in Fig. 8. In turn, this causes the slope of f at x^* to change. Unfortunately, it is not possible to obtain an expression for the probability distribution of $\langle f(x^*)\rangle$ given the probability distribution of the fluctuations affecting the parameter (c or k). Instead, numerical computations of the average $\langle f(x^*)\rangle_\xi \equiv \langle\beta\rangle_\xi$ were done using Gaussian distributed noise of the same standard deviation as used in

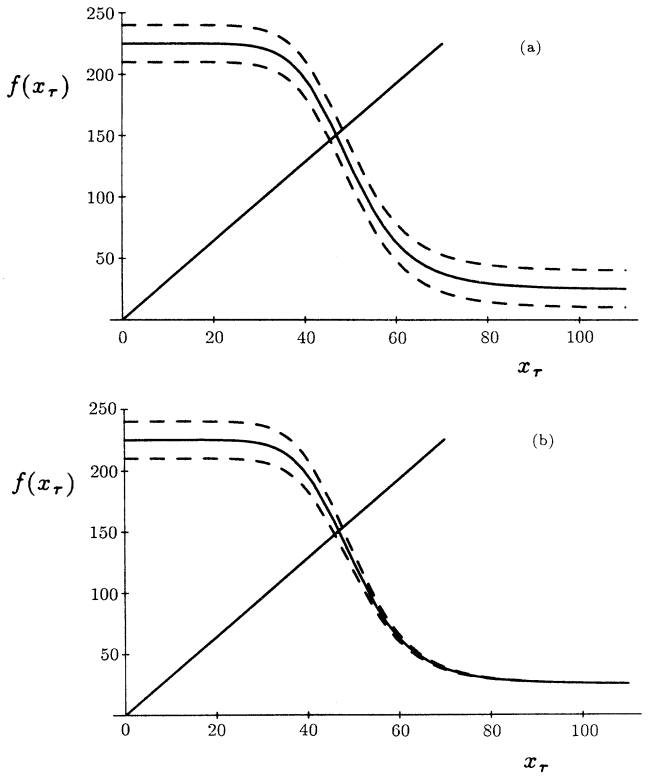

FIG. 8. Plot of the negative feedback function f vs its argument $x(t-\tau)$ in the presence of (a) additive and (b) multiplicative noise. The solid line is the deterministic curve, while the dashed lines show the effect of the noise on f. The fixed point is determined by the intersection of f with the function $y(x)=\alpha x$, where $\alpha=3.21$.

the stochastic simulations of Eq. (1). Because the evolution of the noise process is decoupled from that of the system, all that is necessary is to insure that the noise takes each value in its domain with the proper (Gaussian) probability; t_c is thus not important. $\langle\beta\rangle_\xi$ is plotted against n in Fig. 9 for four delays used in this study: 0.3, 1.5, 10, and ∞, along with the deterministic value of β (solid line). Only the range of values of n over which the averages are computed changes from one plot to the next.

The results clearly indicate that $\langle\beta\rangle_\xi$ can signal the growth of the order parameter. In fact, Fig. 9 shows that $\langle\beta\rangle_\xi$ crosses the solid line at a given value of n, for either additive or multiplicative noise. Further, these crossings occur for values of n close to those corresponding to the onset of growth of the order parameter in Figs. 4–7. While simulations at a greater number of values of n (especially for $\tau=10$) could be done to pinpoint the crossing with accuracy, our calculation is sufficiently precise for illustrating the point of this section. For example, compare Fig. 4(b), $\tau=0.3$, $\sigma=7$, for which the onset is around $n=8.3$ with Fig. 9(a), where the crossing occurs around $n=8.3$. Also, for the map, the crossing occurs at $n=2.855$ in Fig. 9(d) and the order parameter becomes nonzero around $n=2.86$ [result not shown, computed using 10^6 iterates of the map in Eq. (3)]. The only exception is for $\tau=\infty$, for which only the multiplicative noise curve crosses the solid line, and for $\tau=0.1$ (not shown) for which neither type of noise produces a crossing. The absence of crossing for $\tau=\infty$ with additive noise may be due to the fact that not enough values of n between 2.85 and 2.86 (where the crossing is expected) have been used in the computation. A finer sampling indicates in fact that the distance between the curves is minimum around the bifurcation value $n_0=2.84$ and also shows a minimum at $n=2.86$. Since the shifts are very small to begin with, it is conceivable that the curve crosses only briefly if at all, and much better statistics are needed to settle this question.

The rationale behind this calculation is the following. According to Eq. (6), the fixed point is unstable when β is sufficiently negative. If the effect of the noise is to cause β to be less negative on average than without noise, then one might expect, in the real simulation where the noise time scale interacts with the period and radial relaxation time onto the limit cycle, that the system be more stable and thus have a unimodal invariant density. Thus, it is only when $\langle\beta\rangle_\xi$ becomes smaller than the deterministic value at some n that the system actually does become unstable in a statistical sense and exhibit bimodal densities. In the simulation of the stochastic DDE, one would expect the invariant density to depend on the noise, provided the noise fluctuates slowly enough (large t_c) or that radial relaxation onto the limit cycle is fast enough. If this were not the case, the system would not have time to sense the new roots of the characteristic equation, and could not react to the stability increases of x^* by spending more time near x^*. When t_r is small, the oscillation condition can then equilibrate to the fluctuations, and through $\langle\beta\rangle_\xi$ be a good indicator of onset.

This reasoning is substantiated by the following observation. The indicator of onset proposed in this section performs well when the values of n at which the crossing occurs are compared to those at which onset is estimated to occur from the plots in Figs. 4–7, as long as the noise

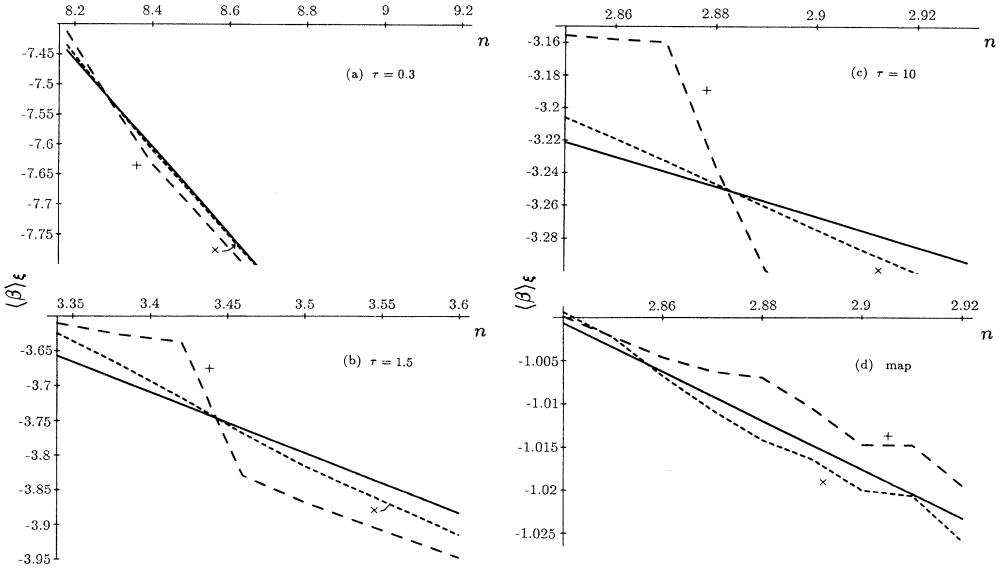

FIG. 9. Plot of the average value of the slope of the feedback function at the fixed point, $\langle\beta(x^*)\rangle$, vs the bifurcation parameter n at four different delays: (a) $\tau=0.3$, (b) $\tau=1.5$, (c) $\tau=10$, and (d) the singular limit where the DDE behaves like a map. The solid curve denotes the deterministic value of the slope, the finely dashed curve corresponds to multiplicative noise, and the coarsely dashed curve to additive noise. The noise standard deviation is $\sigma=7$. The values of n at which the dashed curves intersect the solid curve are to be compared with those at which oscillation onset occurs in the corresponding DDE's in Figs. 4–7. At each value of n, 2×10^6 iterates of the noise process were used in computing the average slope, after discarding the first 1000 iterates.

correlation time is not too short. In fact, for $t_c=0.01$, the shifts are always very small and onset occurs at lower values of n than those at which the crossings occur in Fig. 9. For larger t_c, the shifts are roughly of the same order, as discussed in Sec. V. Thus, if the fluctuations of the Ornstein-Uhlenbeck process are not too fast, especially in comparison with the radial relaxation time t_r, which was shown in Sec. III to be an increasing function of the delay, then the indicator seems to work well. It is then more surprising that the indicator does not work for $\tau=0.1$, for which t_r is small. This may be due to the fact that the indicator works in the absence of major nonlinearities, and this is certainly not the case for $\tau=0.1$ for which the Hopf bifurcation occurs when the feedback function is very nonlinear.

In Fig. 9, the crossings for additive and multiplicative noise occurs almost at the same value. Hence, more extensive simulations may allow us to predict from the behavior of this indicator whether the additive or multiplicative shifts are greater. Clearly, $\langle\beta\rangle_\xi$ gives only a rough estimate of the postponement across a variety of conditions, although it performs surprisingly well under certain conditions. More work is needed to clarify how the knowledge of the behavior of $\langle\beta\rangle_\xi$ can be combined with the other time scales in the DDE to predict a given postponement.

We have verified that $\langle\beta\rangle_\xi$ is also a good indicator of oscillation onset at higher noise intensities ($\sigma=15$) for $\tau=0.3$, but not as good at the other delays. Thus it seems that this quantity is useful only for low noise intensities and for larger delays. In fact, once the crossing has occurred, reverse crossings were found at higher values of n. This points to the fact that this quantity may be relevant to the stochastic onset of oscillation only locally (i.e., in some linear range). We have also computed a "stochastic oscillation condition" using Eq. (6) with $\langle f(x^*)\rangle$ substituted for β. The fulfillment of the inequality in this case did not prove to be a signature for the behavior of the order parameter. We have also looked at the peak of the distribution of $\beta(\xi)$ rather than its mean $\langle\beta\rangle_\xi$, to see whether the system decides to bifurcate based on the time spent in each state or whether it cares about the time average $\langle\beta\rangle$. The distributions are in fact slightly skewed, being typically broader for multiplicative than for additive noise of the same standard deviation. The mean was found to provide a better indication of the onset than the mode. These results may depend on the particular choice for α.

VIII. DISCUSSION

This work is a thorough investigation of the behavior of a first-order DDE with additive and multiplicative noise at a Hopf bifurcation. We have argued in Secs. I and II that this class of equations is important in various applications. The results of this study are valid for systems that can undergo a Hopf bifurcation, regardless of whether they bifurcate further into chaos, as for the Mackey-Glass equation and the Ikeda equation, or not, as in the simple negative feedback case considered here. The results should be useful for delayed feedback systems in which the gain varies, as occurs, e.g., in lasers and in physiological control systems. Our study has revealed a variety of behaviors, some of which have been explained by considering the stochastic behavior of limiting cases of the DDE (ODE's and maps). Insight into the origin of the postponements of the Hopf bifurcation at different delays, noise correlation times, and intensities has further been obtained by looking at the behavior of a special indicator (Sec. VII), the average of the slope of the feedback function at the fixed point. It remains to be seen whether equivalent quantities can be found for noise-induced transitions in ODE's, or if this is only a property of DDE's.

Many studies of DDE's have focused on the question of how many degrees of freedom interact in the chaotic regime as a function of the delay. Very little is known about the effective number of degrees of freedom there are at low delays for simple periodic motion. It is known, however [39], that approximations to DDE's in terms of integro-differential equations (which model a distributed rather than a fixed delay) must be at least three dimensional in order to undergo a Hopf bifurcation. This would suggest that even as the delay becomes small, the system has at least three degrees of freedom, as suggested in Sec. III and at the end of Sec. IV. When the delay is small, the feedback function is very nonlinear. It appears in this case that it is not possible to expand the DDE in powers of τ or $\alpha\tau$ and obtain an ODE that can oscillate autonomously, for this could only yield a first-order ODE. On the other hand, although it has been reported that many properties of DDE's do not carry over to the map due to the singular limit [9], our study gives an example of a smooth transition between the noisy behavior of the map and that of the DDE. In fact, the additive and multiplicative shifts decrease with increasing delay and further become roughly equal, which are both properties of the map.

Our study has compared postponements of the Hopf bifurcation with additive and multiplicative noise using the simplest order parameter, the separation of the maxima of the invariant density. Other order parameters are possible, e.g., the rms amplitude [38]. One might even consider constructing three-dimensional densities $P(x(t),x(t-\tau))$ and applying the criterion proposed in Ref. [26]. While this type of calculation is very computer intensive and is beyond the scope of the present paper, the application of such criterion may provide insights into the behaviors found in our work (i.e., why, in Sec. IV, there is a crossover of the shifts for large and not small t_c). Analog computation should probably be used to resolve this issue.

There has been work on the application of Fokker-Planck theory to DDE's in another context than the one of this paper, that of analyzing the chaos produced by DDE's [40]. This work views DDE's in chaotic regimes as generators of colored noise. This approach, in which Kramers-Moyal expansions are performed to obtain approximations to the invariant densities, works only for large delays or for feedback functions that strongly decorrelate their inputs, e.g, when $f(x_\tau)\propto\sin(Ax)$, where $A\gg1$. These conditions are not applicable to our case, although it would be interesting to evaluate terms in

such an expansion by computing the correlation functions numerically. An important issue to address eventually is whether there exists a unique invariant measure for stochastic DDE's. Although one strongly suspects that such a measure (supported on the domain of x) exists for simple periodic behaviors, based on numerical simulations that scan, due to the noise, elements of the Banach space of initial conditions, they may not be unique when chaos interacts with noise due to the multistability known to occur in the deterministic case [7].

In view of the dearth of analytical tools to study stochastic DDE's, the patterns found in our results should provide encouragement to undertake such analytic studies. The time appears ripe to tackle the problem of performing a center manifold reduction for the stochastic version of Eq. (1) by extending the techniques of functional differential equations to the stochastic case [41]. *A priori*, center manifold reductions for the stochastic DDE may be in the short term a more fruitful avenue than reductions on a Fokker-Planck-type equation, because they will avoid the problem of having to define densities in a Banach space. Once the former reduction is performed, the construction of a standard Fokker-Planck equation in two dimensions, or higher if the noise is colored, could proceed as in the case of stochastic ODE's.

ACKNOWLEDGMENTS

The author has greatly benefited from discussions with Michael Mackey, Frank Moss, Ivan L'Heureux, and Doyne Farmer. The author further wishes to acknowledge financial support from the Natural Sciences and Engineering Research Council of Canada, from the Complex Systems Group and the Center for Nonlinear Studies at Los Alamos National Laboratory, and from NATO through Grant No. CRG-901027.

[1] K. Ikeda, Opt. Commun. **39**, 257 (1979).
[2] M. W. Derstine, H. M. Gibbs, F. A. Hopf, and D. L. Kaplan, Phys. Rev. A **26**, 3720 (1982).
[3] G. E. Hutchison, Ann. N. Y. Acad. Sci. **50**, 221 (1948).
[4] M. C. Mackey and L. Glass, Science **197**, 287 (1977).
[5] J. D. Farmer, Physica **4D**, 366 (1982).
[6] M. Le Berre, E. Ressayre, A. Tallet, and H. M. Gibbs, Phys. Rev. Lett. **56**, 274 (1986).
[7] K. Ikeda and K. Matsumoto, Physica **29D**, 223 (1987).
[8] P. Nardone, P. Mandel, and R. Kapral, Phys. Rev. A **33**, 2465 (1986).
[9] J. Mallet-Paret and R. D. Nussbaum, in *Chaotic Dynamics and Fractals,* edited by M. F. Barnsley and S. G. Demko (Academic, Orlando, 1986).
[10] S. N. Chow and J. Mallet-Paret, in *Coupled Nonlinear Oscillators,* edited by J. Chandra and A. C. Scott (North-Holland, Amsterdam, 1983).
[11] K. Ikeda, K. Kondo, and O. Akimoto, Phys. Rev. Lett. **49**, 1467 (1982).
[12] L. Stark, J. Opt. Soc. Am. **52**, 925 (1962); J. P. H. Reulen, J. T. Marcus, M. J. van Gilst, D. Koops, J. E. Bos, G. Tiesinga, F. R. de Vries, and K. Boshuizen, Med. Biol. Eng. Comp. **26**, 27 (1988).
[13] A. Longtin, J. G. Milton, J. E. Bos, and M. C. Mackey, Phys. Rev. A **41**, 6992 (1990).
[14] A. Longtin and J. G. Milton, Bull. Math. Biol. **51**, 605 (1989).
[15] W. Horsthemke and R. Lefever, *Noise Induced Transitions: Theory and Applications in Physics, Chemistry and Biology,* edited by H. Haken, Springer Series in Synergetics Vol 15 (Springer, Berlin, 1984).
[16] H. Risken, *The Fokker-Planck Equation,* 2nd ed., edited by H. Haken, Springer Series in Synergetics Vol. 18 (Springer, Berlin, 1989).
[17] M. Schumaker, Phys. Lett. A **122**, 317 (1987).
[18] E. Knobloch and K. A. Wiesenfeld, J. Stat. Phys. **33**, 611 (1983).
[19] F. Baras, M. Malek Mansour, and C. Van den Broeck, J. Stat. Phys. **28**, 577 (1982).
[20] C. Nicolis and G. Nicolis, Dynam. Stabil. Syst. **1**, 249 (1986).
[21] R. Lefever and J. Wm. Turner, Phys. Rev. Lett. **56**, 1631 (1986).
[22] M. C. Mackey, A. Longtin, and A. Lasota, J. Stat. Phys. **60**, 735 (1990).
[23] S. Kabashima and T. Kawakubo, Phys. Lett. **70A**, 375 (1979).
[24] R. Graham, Phys. Rev. A **25**, 3234 (1982).
[25] S. T. Ariaratnam and N. Sri Namachchivaya, in *Dynamical Systems Approaches to Nonlinear Problems in Systems and Circuits,* edited by F. M. A. Salam and M. L. Levi (Society for Industrial and Applied Mathematics, Philadelphia, 1988), p. 39.
[26] L. Fronzoni, R. Mannella, P. V. E. McClintock, and F. Moss, Phys. Rev. A **36**, 834 (1987).
[27] M. San Miguel and S. Chaturvedi, Z. Phys. B **40**, 167 (1980).
[28] L. Schimansky-Geier, A. V. Tolstopjatenko, and W. Ebeling, Phys. Lett. **108A**, 329 (1985).
[29] I. L'Heureux and R. Kapral, J. Chem. Phys. **90**, 2453 (1989).
[30] G. Yin and K. M. Ramachandran (unpublished); B. S. White, Commun. Pure Appl. Math. **XXIX**, 113 (1976).
[31] V. B. Kolmanovskii and V. R. Nosov, *Stability of Functional Differential Equations,* Vol. 180 of *Mathematics in Science and Engineering Series* (Academic, Orlando, 1986).
[32] H. W. Stech, J. Math. Anal. Appl. **109**, 472 (1985).
[33] In the case where $\alpha\tau \to \infty$ because $\alpha \to \infty$, the ratio f/α must be kept constant in taking the limit.
[34] J. Guckenheimer and P. Holmes, *Nonlinear Oscillations, Dynamical Systems, and Bifurcations of Vector Fields* (Springer, New York, 1983).
[35] R. F. Fox, I. R. Gatland, R. Roy, and G. Vemuri, Phys. Rev. A **38**, 5938 (1988).
[36] A. Longtin (unpublished results).
[37] J. P. Crutchfield, J. D. Farmer, and B. A. Huberman, Phys. Rep. **92**, 45 (1982).
[38] S. J. Linz and M. Lücke, Phys. Rev. A **33**, 2694 (1986).
[39] R. Vallée and C. Marriott, Phys. Rev. A **39**, 197 (1989); A. Longtin, in Proceedings of the 3rd Neural Information Processing Systems Conference, Denver, Nov. 1990, edited by R. P. Lippmann, J. E. Moody, and D. S. Touretzky (Morgan Kaufmann, San Mateo, CA, 1991).
[40] M. Le Berre, E. Ressayre, A. Tallet, and Y. Pomeau, Phys. Rev. A **41**, 6635 (1990).
[41] J. K. Hale, *Theory of Functional Differential Equations* (Springer, New York, 1977).